Event Name

Paper Number (SPE-123456) or Manuscript ID

Tackling Subsurface Complexity in Middle East Seismic Imaging - Use or Remove Shear Arrivals?

J. Brittan[1], J. Kumar[2], and M. Raafat[3*]

[1]TGS, Weybridge, United Kingdom
[2]TGS, Kuala Lumpur, Malaysia
[3]TGS, Cairo, Egypt

Introduction

In areas with high impedance contrast reflectors, which are common offshore in the Middle East, the stark contrast between high-velocity formations (typically salt or carbonates) and the surrounding sediments often gives rise to converted wave modes. These occur when compressional (P-wave) energy transforms into shear (S-wave) energy upon encountering the sharp velocity boundaries at the top or base of a high-velocity body. Since S-waves travel more slowly than P-waves, their arrival times differ, and they can appear as misleading deeper events in seismic records. If not properly managed, this energy can obscure true reflections and hinder accurate subsurface interpretation (Elbassiony *et al*., 2018).

For example, one of the main challenges in hydrocarbon exploration within the Messinian salt province of the Eastern Mediterranean is the contamination of P-wave seismic images by these converted wave modes. In this region, the salt typically has interval velocities around 4200–4300 m/s, while adjacent post- and pre-Messinian sediments range from 2400 to 3000 m/s (Jones and Davison, 2014). This sharp velocity contrast promotes mode conversion, especially at steep salt boundaries, often resulting in complex interference patterns in seismic data. While converted waves can occasionally improve subsurface illumination or provide additional geometric insight, they more often act as noise—particularly problematic for imaging sub-salt targets where precision is crucial. This leads to the dilemma for the imaging geophysicist, shall we use the information provided by these shear arrivals or remove these arrivals as noise? Whilst emerging technologies such as elastic FWI tantalisingly offer the opportunity to exploit the information carried by the shear wave arrivals, in exploration areas with little well control, there are likely to be significant uncertainties in shear velocity information (especially in the shallow subsurface) that may hinder this approach. Thus, for the purpose of this paper we will be generally looking at ways of attenuating these unwanted arrivals – without harming the underlying primary arrivals.

Among the various types of converted waves, those involving conversion at both the top and base of the salt—such as PSPP and PPSP modes—are especially problematic due to their strong amplitudes and complex moveout behaviour. Symmetrical conversions like PSSP, although theoretically possible, are rarely observed in practice due to their weaker amplitudes and longer travel times. Traditional suppression techniques, such as velocity-based filtering or targeted muting using travel-time models, often fall short in regions with complex or irregular salt geometries.

To more effectively address these issues, we investigate a modelling-based attenuation method that leverages dual acoustic simulations. This involves running two 3D acoustic models—one that includes the base salt interface and another that excludes it—to isolate the energy associated with converted waves (Kumar *et al*., 2018). The synthetic data generated allows for a more precise estimation of the converted wavefield, which can then be subtracted from the original data before migration. This technique offers a more robust suppression of mode-converted noise, particularly in geologically complex settings.

In this paper, we apply this modelling-based strategy to newly acquired multisensor seismic datasets from the Eastern Mediterranean. The results demonstrate that this approach significantly enhances image clarity, supports amplitude-preserving processing workflows, and improves the accuracy of velocity model building in areas affected by strong P-to-S wave conversions.

Method

In areas littered with high-impedance contrast geobodies (such as salt or carbonates), converted mode contamination remains a persistent challenge to accurate P-wave seismic imaging. Sharp acoustic impedance contrasts at salt-sediment boundaries lead to P-to-S wave conversions, producing modes such as PSPP, PPSP, and PSSP. These converted waves typically re-enter surrounding sediments as P-waves, arriving with delayed travel times. Their presence degrades image quality, hampers interpretation, and often obscures sub-salt targets. While converted modes can occasionally enhance illumination due to broader angular coverage, they are more commonly treated as coherent noise that needs to be attenuated to improve image clarity.

Key converted wave types (Figure 1) include:

- **PSPP**: P-wave down, S-wave through salt, P-wave up
- **PPSP**: P-wave down and S-wave up
- **PSSP**: S-wave on both downgoing and upgoing paths

Among these, PSSP modes typically arrive significantly later and with weaker amplitudes, due to the slower speed of S-waves and lower velocity contrast between S-wave salt and surrounding P-wave sediments. As a result, PSSP energy is often not visible in field data and is generally not modelled.

Traditional suppression methods rely on:

- **Normal move-out (NMO) velocity filtering** to exploit the lower apparent velocity of converted waves (Ogilvie and Purnell, 1996)
- **Travel-time muting** using ray tracing (Lu *et al*., 2003)

However, these methods are less effective in areas with complex salt geometries. Dual-leg 3D acoustic modelling (Huang *et al*., 2013) has been proposed to simulate converted wave energy for subtraction from either pre- or post-migration data. Yet, in complex settings, top-salt diffractions can interfere with converted energy from the base salt, complicating forward modelling and limiting subtraction effectiveness.

To address this, we apply two separate 3D acoustic modelling simulations (Kumar *et al*., 2018): one including the base salt interface, and one excluding it. Subtracting the latter from the former yields a cleaner converted wavefield, isolating energy generated at the base salt and minimizing top-salt diffraction contamination. This enables more accurate removal from both pre-stack and pre-migration gathers.

To determine which converted modes to model, we use the **diagnostic ratio**:

- For **asymmetrical modes (PSPP, PPSP)**:

$$r = 2\frac{v_s}{v_p - v_s}, \quad (1)$$

- For **symmetrical mode (PSSP)**:

$$r = \frac{v_s}{v_p - v_s}, \quad (2)$$

Typically, the ratio ranges between 2–3 for asymmetrical modes and 1–1.5 for symmetrical modes. In this study, a ratio of approximately 2.2 indicates that PSPP and PPSP are the dominant contributors, guiding our forward modelling choices.

The suppression workflow involves:

1. **Building a P-wave velocity model** with detailed salt geometry.
2. **Creating an S-wave velocity model** within the salt, by scanning for the velocity that flattens converted mode events at the base salt.
3. **Running two 3D acoustic models**:
    - The first includes both top and base salt interfaces.

- The second excludes the base salt interface.

4. **Subtracting the second modelled dataset from the first**, isolating converted energy from the base salt.

This differential modelling approach effectively removes overlapping top-salt diffractions, enabling targeted suppression of PSPP and PPSP energy.

Adaptive subtraction is then performed using a hybrid method:

- **Least-squares filtering in the time-space domain**
- **Curvelet-domain subtraction** for improved coherence and preservation of primary reflections

This ensures only the modelled converted energy is removed, preserving critical reflection events for interpretation (Perrier *et al*., 2017).

While converted wave suppression can also be performed in the image domain using just the first model, top-salt diffractions may obscure converted events pre-migration. The differential modelling approach facilitates earlier and cleaner separation in the data domain, enhancing suppression effectiveness.

Overall, this method achieves reliable attenuation of converted energy while preserving primary reflections, making it highly effective in structurally complex environments where sub-salt illumination is essential for exploration success.

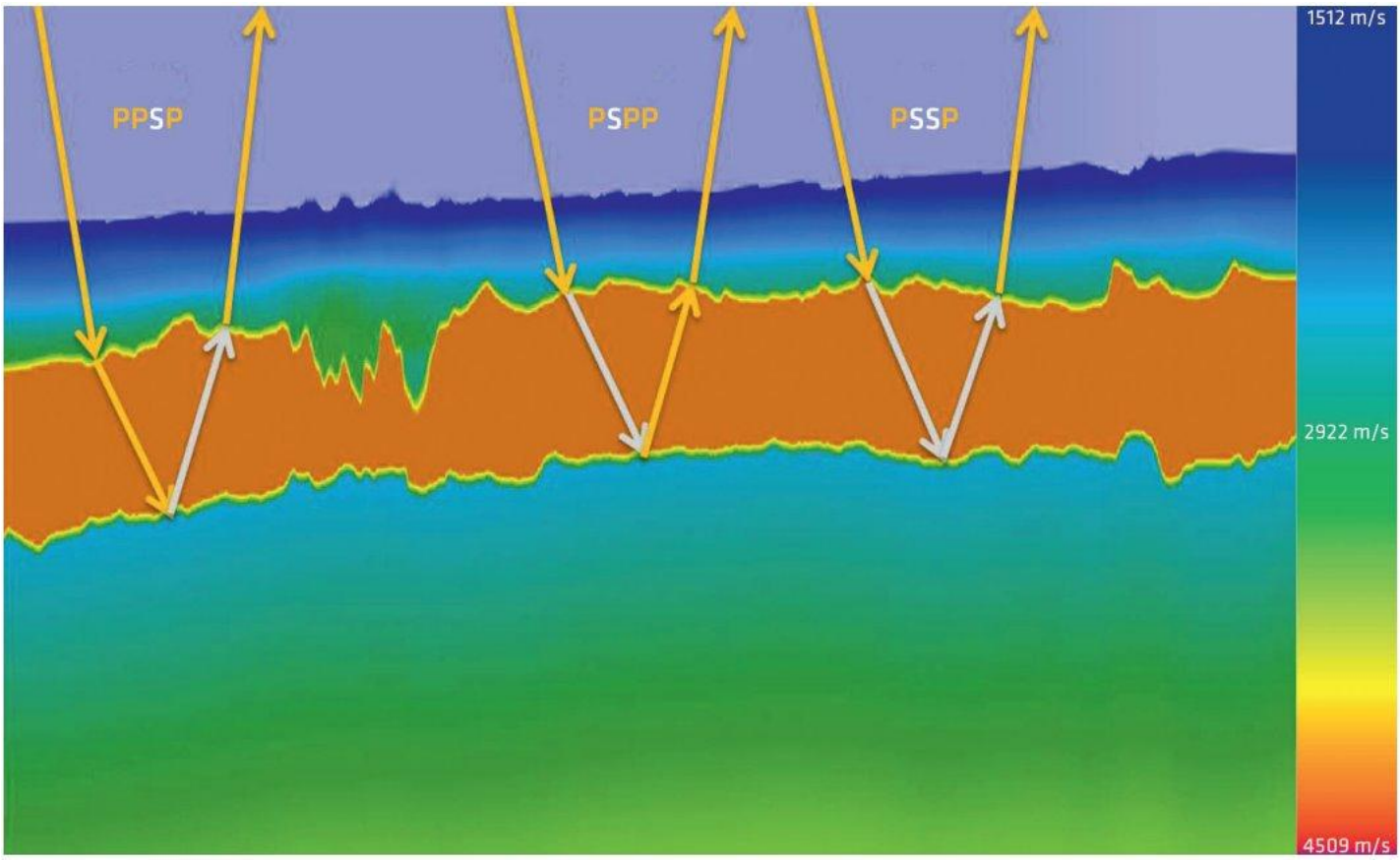

Fig. 1 – The possible ray paths of converted waves from the salt layer. The colour scale, in this diagram, refers to the P-wave velocity.

Examples

The seismic data examples that are shown in this paper were acquired as part of a multi-client campaign in the Eastern Mediterranean Sea, offshore Egypt, with water depths ranging from 200 m to 3000 m. The methodology described above was applied where the converted mode energy was causing significant interference to the primary energy – this was typically in the thickest salt sections. The modelling of symmetrical modes (PSSP) was ignored in the cases described below, owing to a lack of evidence of its presence in the recorded field data. The ratio (r), described in equations (1) and (2), was estimated at 2.2, inferring that this converted mode was

composed of a wave with only one of the up-coming or down-going wave-fields as an S-wave in the salt layer; either PSPP, or PPSP, or both.

Example 1

The survey was acquired using a triple-source configuration and twelve 10 km long multisensor streamers at a depth of 20 m separated by 150 m. The nominal seismic acquisition bin size was 6.25 m by 25 m, with 100-fold coverage. The water depth lies between 2000m amd 3000m.

The velocity model for the modelling was generated using reflection tomography in the post-salt section to estimate the sediment velocity. The salt layer velocity was estimated using a salt flooding methodology after interpreting the top salt reflector. The aim of this flooding step was to estimate the P-wave velocity that produces optimal flatness of the base salt reflection. The S-wave velocity was obtained by scanning for the velocity which flattens the converted mode energy at the same depth as the interpreted base salt. For this dataset, the P-wave velocity of the salt was estimated at 4200 m/s, whereas the S-wave velocity was estimated at 2200 m/s. FWI was used in the velocity model building workflow, but it was not included in the velocity model for converted waves modelling. Figure 2 shows the shot gathers with and without the proposed converted wave attenuation flow. The arrow shows the location in shot gather where the converted wave was recorded in data domain. Figure 2 clearly shows effective attenuation of the recorded converted wave.

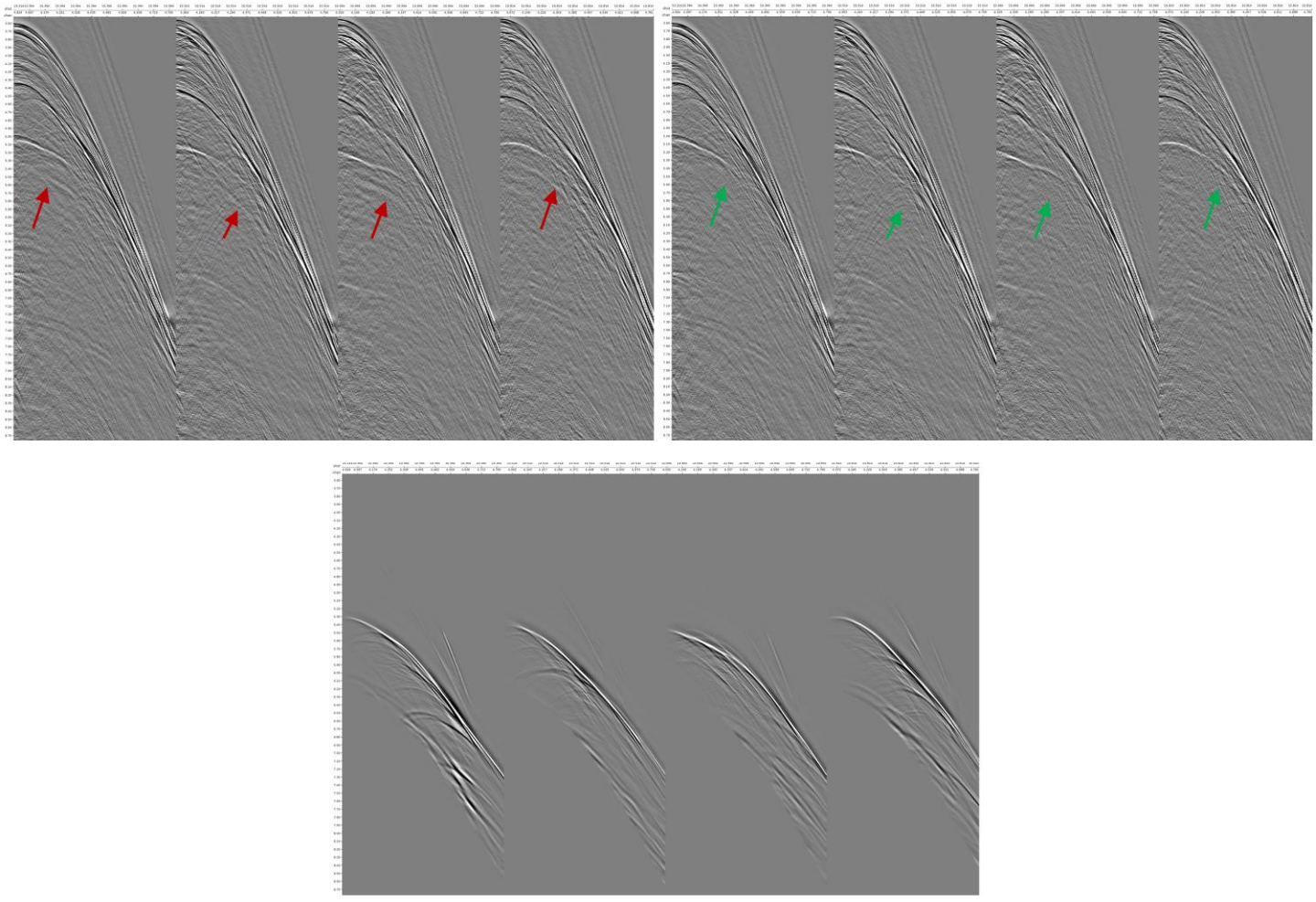

Fig. 2 – Common Shot Gathers without converted wave attenuation flow applied (top left), with converted wave attenuation flow applied (top right) and the Converted wave model (bottom).

Whilst the shot gathers show some indication of the converted waves, Figure 3 shows that the converted wave energy can be more easily identified in the pre-migration stack. Examining both the top and base of the salt in the stack reveals the complexity of the salt layer, which adds further challenges to accurately modeling and subtracting the converted wave energy. The arrows highlight the locations of the recorded converted wave energy on the pre-migration stack section. It is evident that the proposed workflow has effectively attenuated the converted wave energy. The image domain QC, on migrated stack obtained using a Kirchhoff pre-stack depth migration, is shown in figure 4, highlighting the effective attenuation of the converted wave in such complex salt regime. The difference display shows a good isolation of the converted wave event.

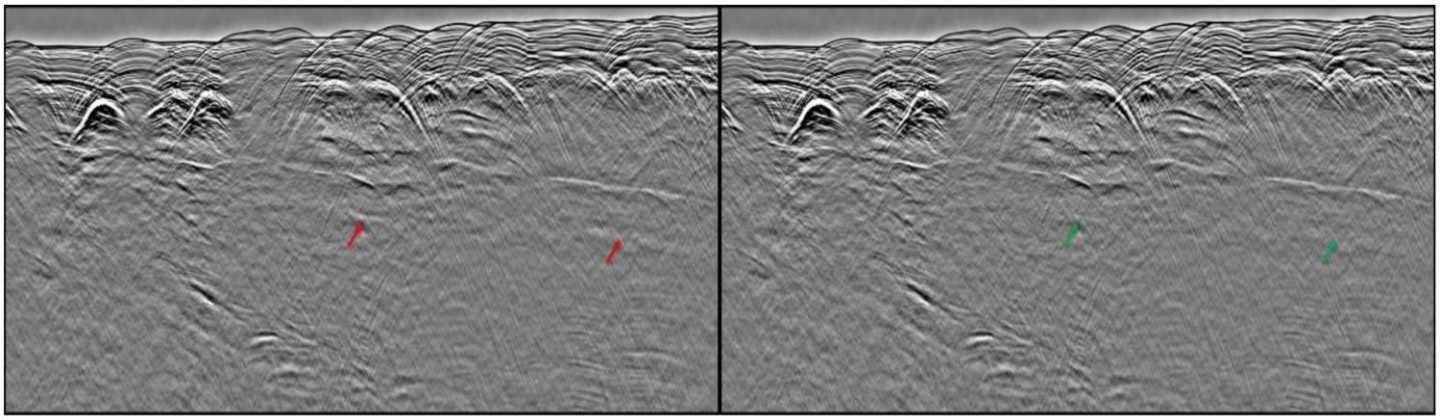

Fig. 3 – Unmigrated stack without converted wave attenuation flow (left) and with converted wave attenuation flow (right).

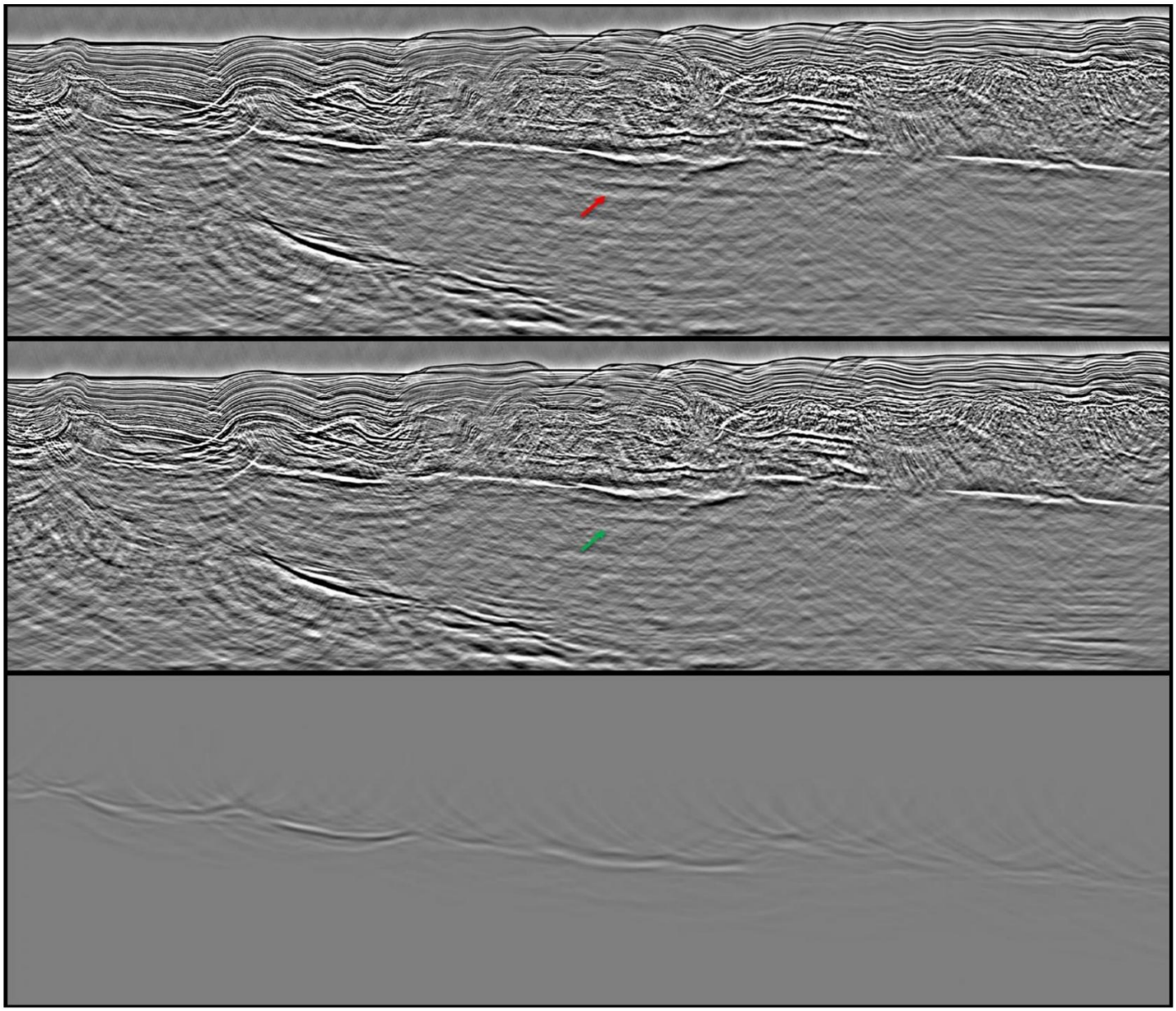

Fig. 4 – Image domain stack obtained by a Kirchhoff migration without converted wave attenuation flow (top) and with converted wave attenuation flow (middle) and the difference display (bottom).

Example 2

This example is from a survey acquired with a configuration using 12 multisensor streamers, each 10000-m long, three source arrays were used shooting at an interval of 16.667 m. The nominal seismic acquisition bin size was 6.25 m by 25 m. A similar velocity model building approach to example 1 was undertaken in which reflection tomography is used in the post-salt section to estimate the sediment velocity, and the salt layer velocity was estimated using a salt flooding methodology after interpreting the top salt reflection. Base salt interpretation was performed to constrain the salt layer using appropriate salt velocity obtained from salt flood methodology.

Figure 5 shows a common shot gather and stack in data domain from the survey area annotated with the location of the asymmetrical mode converted energy, and results after the mode converted energy has been removed. The effectiveness of the converted energy removal is clearly visible in the data domain. Figure 6 shows Kirchhoff depth stack images before and after the removal of the mode converted energy. The absence of the converted wave in the middle of the migrated stack is attributed to the salt pinching out, resulting in no interface for mode conversion.

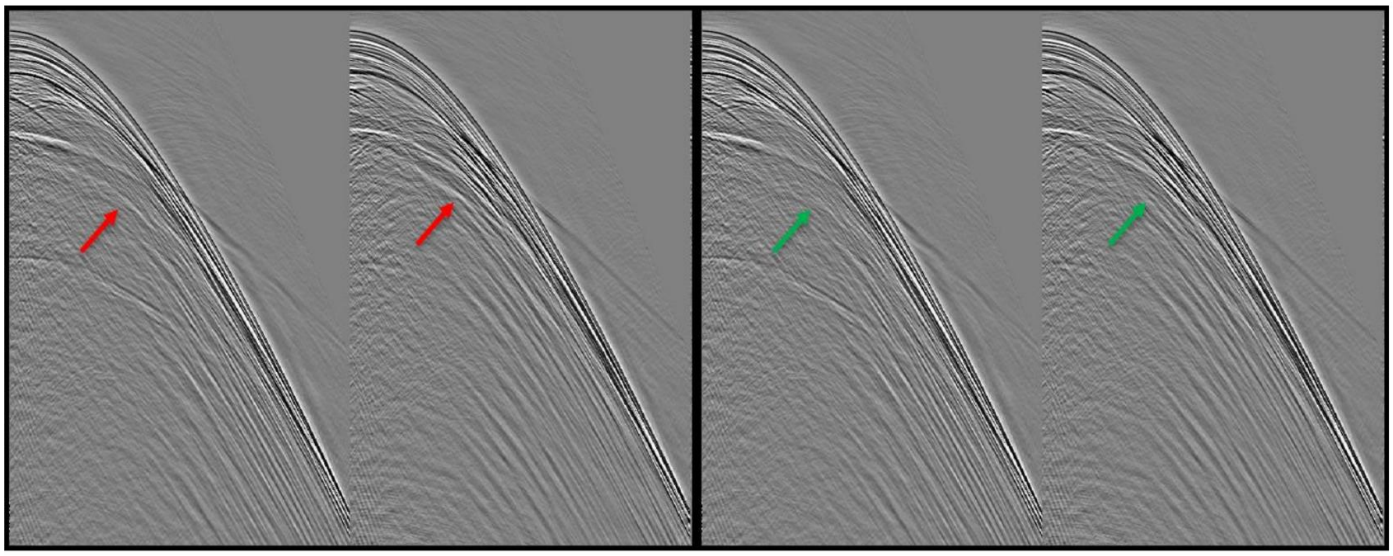

Fig. 5 – Common Shot Gathers without converted wave attenuation flow applied (left) and with converted wave attenuation flow applied (right).

Example 3

In this example the acquisition parameters are very similar to the previous survey with a triple-source configuration and twelve 10 km long multisensor streamers at a depth of 20 m separated by 150 m. The nominal seismic acquisition bin size was 6.25 m by 25 m, with 100-fold of coverage.

The velocity model used for the converted wave modeling was derived through tomography focused on the post-salt section to estimate sediment velocities. During the salt body velocity analysis, certain areas were identified as containing so-called “dirty” salt, which required a lower average velocity compared to regions of “clean” salt. A spatially varying salt velocity was implemented, using a background clean salt velocity of 4400 m/s, while assigning slower velocities in the dirty salt regions to optimize gather flatness at the base of the salt.

Within this large exploration area, the composition of Messinian salt varied significantly from thick, pure salt in the northwest to a more contaminated, mixed salt in the southeast. This variation had a notable impact on the observable converted wave in the dataset. In areas with cleaner salt, the converted wave appeared stronger and more continuous, whereas in regions with dirty salt, the converted wave energy weakened and became less visible in seismic data.

To explore the link between converted wave coherency and salt purity, Figure 7 presents a comparison between a converted wave amplitude map and a salt dirtiness map. The converted wave coherency map was generated by calculating the RMS amplitude within a ±100 ms window around the expected converted wave arrival time. For the salt dirtiness map, the RMS amplitude was calculated from 100 ms below the top salt boundary to 100 ms above the base salt. A stronger amplitude within the salt layer indicates more dirtiness within Messinian salt. As shown in Figure 7a, the converted wave is stronger and more continuous in the western areas, which correspond

to regions of cleaner salt in Figure 7b. In contrast, Figure 7b exhibits higher salt dirtiness in the eastern regions, corresponding to the presence of weaker converted waves in Figure 7a.

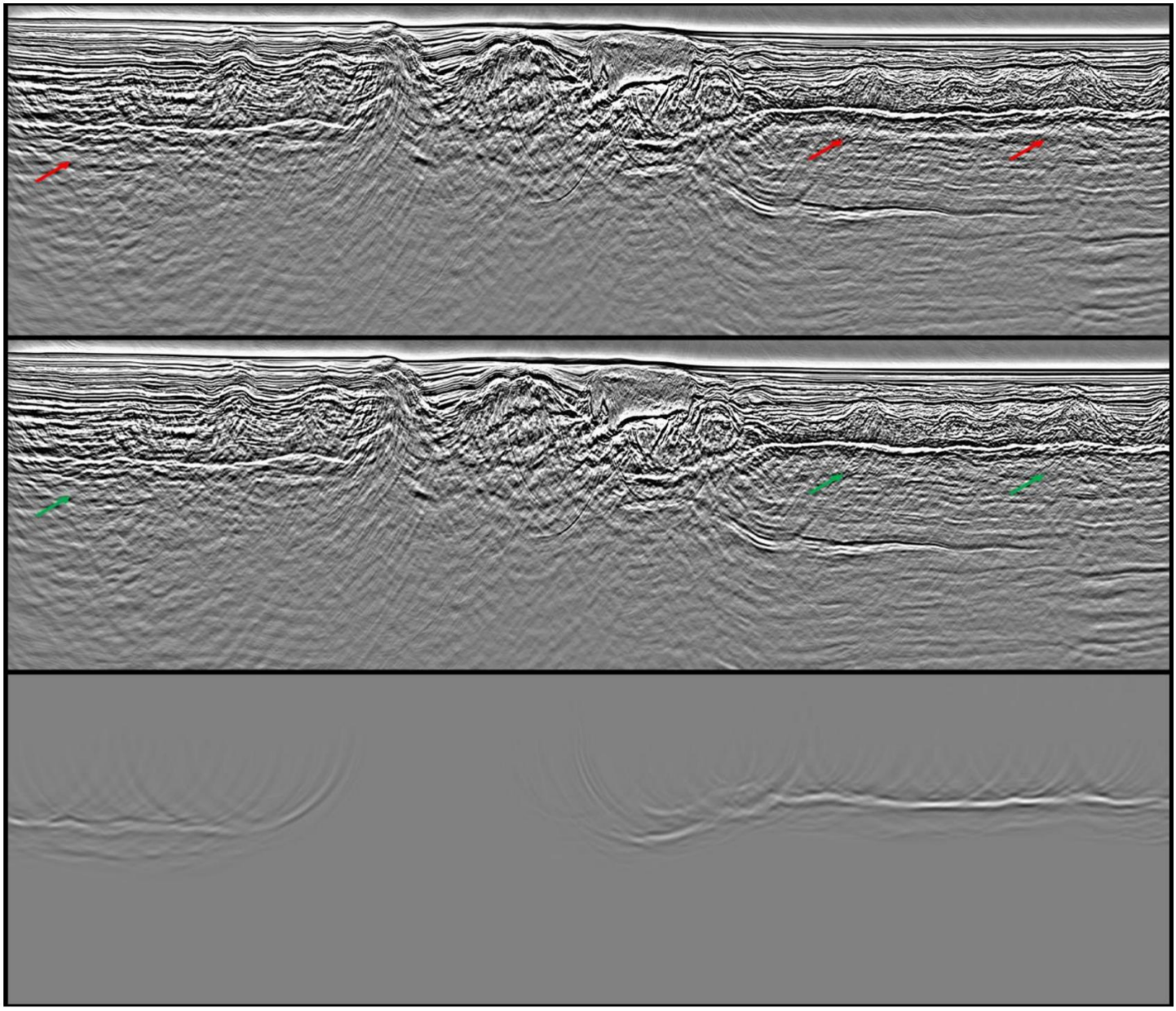

Fig. 6 – Image domain stack obtained by a Kirchhoff depth migration without converted wave attenuation flow (top) and with converted wave attenuation flow (middle) and the difference display (bottom). In the centre of the section, there is a lack of coherent base-salt reflector – leading to an absence of strong coherent converted wave arrivals.

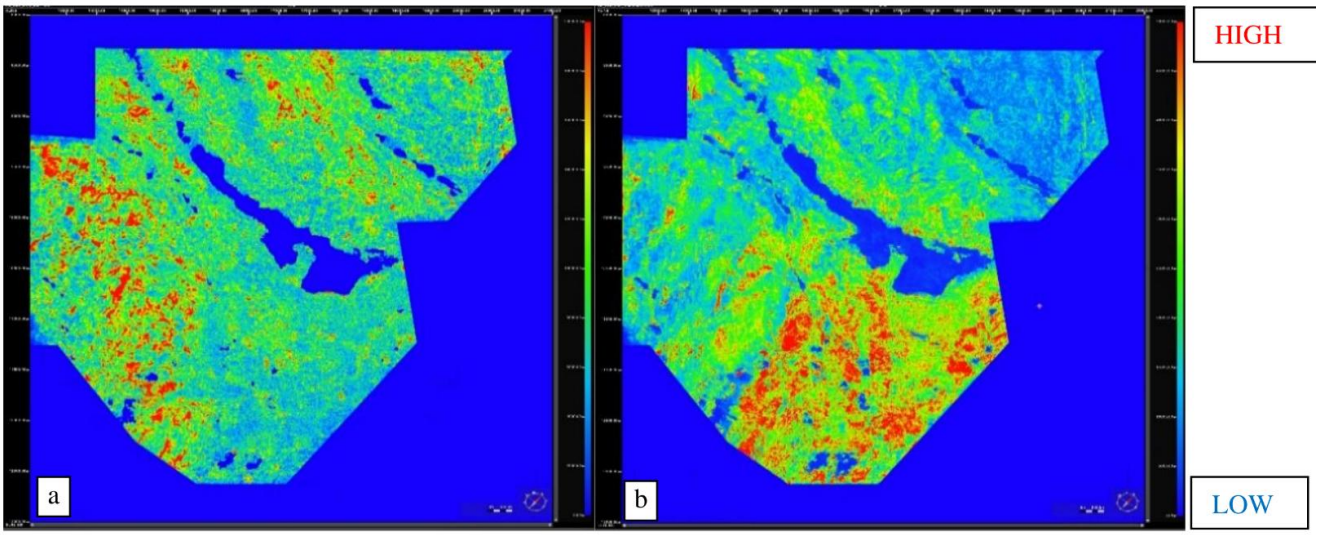

Figure 7: The converted wave coherency map (a) the salt dirtiness map (b). Note the spatial anti- correlation between the two metrics – i.e. a strong converted wave is generally associated with the areas of cleanest salt.

Conclusion

In the Middle East, imaging results are often challenged by high velocity bodies with complex geometries leading to the presence of strong converted-wave energy. Our study, conducted in three separate locations in the Eastern Mediterranean with variable salt complexity, demonstrates that a straightforward yet robust attenuation workflow can effectively suppress both asymmetrical (PSPP, PPSP) or symmetrical (PSSP) converted modes. This enhances pre-salt reflectivity, improves data interpretability, and reduces exploration risk.

In the future, however, the converted-wave energy may be utilized during the imaging itself. Technologies such as elastic multi-parameter full waveform inversion (Huang *et al*., 2025) utilize better approximations to the physical processes governing wave propagation and therefore take into account the information contained in all arriving waveforms. Thus, as these types of approaches become more commonly used, modes such as PSPP, PPSP and PSSP should contribute to the derivation of a full elastic earth model. However, it should always be borne in mind that surface seismic, with limited offsets and azimuths, has variable sensitivity to the various components of a full (anisotropic) elastic earth model (Oh *et al*., 2020). To reduce the size of the null-space in such inversions (especially in areas where little or no *a-priori* information – such as well control, is available), it is likely that the use in the inversion of data from all four components recorded in a typical OBN acquisition will need to be input into the inversion. In fact, to utilize such effects as the polarization of S-waves correctly in the inversion, it may be appropriate to use a new generation of sensors that record both the translational and rotational components of the incoming wavefields (Kritski *et al*., 2025).

Acknowledgements

The authors would like to thank TGS MultiClient for granting permission to present examples from various surveys conducted by TGS across the Mediterranean Sea. Special appreciation goes to the TGS geophysicists whose efforts was instrumental in generating the results.

References

Elbassiony, A., Kumar, J. and Martin, T., 2018. Velocity model building in the major basins of the eastern Mediterranean Sea for imaging regional prospectivity. The Leading Edge, 37(7), 519-528

Huang, Y., W. Gou, O. Leblanc, S. Ji, and Y. Huang, 2013, Salt-related converted-wave modeling and imaging study: 75th Annual EAGE Conference and Exhibition, Tu 01 13.

Huang,G., Macesanu, C., Liu, F., Ramos-Martinez, J., Whitmore, D., Calderon, C. and Bloor, R., 2025. Multiparameter Elastic FWI for Joint Inversion of Velocity and Reflectivity. 86th EAGE Annual Conference & Exhibition, Jun 2025, Volume 2025, p.1 - 5

Jones, I. F., and I. Davison, 2014, Seismic imaging in and around salt bodies: Interpretation, 2, 4, SL1–SL20.

Kritski, A., Westerdahl, H., Pedersen, Å.S., Thompson, M., Ten Kroode, F. and Seher, T., 2025. Utilizing Rotational Data for Seismic Polarization Analysis and Filtering of Vertical Component Data: 86th EAGE Annual Conference & Exhibition, Jun 2025, Volume 2025, p.1 - 5

Kumar, J., Bell, M., Salem, M., Martin, T. and Fairhead, S., 2018. Mode conversion noise attenuation, modelling and removal: case studies from Cyprus and Egypt. First Break, 36, 113–120.

Lu, R. S., D. E. Willen, and I. A. Watson, 2003, Identifying, removing and imaging P-S-conversions at salt-sediment interfaces: Geophysics, 68, 3, 1052–1059.

Ogilvie, J. S., and G. W. Purnell, 1996, Effects of salt-related mode conversions on subsalt prospecting: Geophysics, 61, 2, 331–348

Oh, J-W., Shin, Y., Alkhalifah, T. and Min, D-J., 2020. Multistage elastic full-waveform inversion for tilted transverse isotropic media: Geophysical Journal International, 223, 57-76.

Perrier, S., Dyer, R., Liu, Y., Nguyen T. and Lecocq, P., 2017. Intelligent adaptive subtraction for multiple attenuation. 79th Annual EAGE Conference and Exhibition, We B3 0